Interplay between lattice dynamics and superconductivity in Nb_3Sn thin films

S. Couet,[1,*] H. Peelaers,[2,3] M. Trekels,[1] K. Houben,[4] C. Petermann,[1] M. Y. Hu,[5] J. Y. Zhao,[5] W. Bi,[5,6] E. E. Alp,[5] E. Menéndez,[1] B. Partoens,[3] F. M. Peeters,[3] M. J. Van Bael,[4] A. Vantomme,[1] and K. Temst[1]

[1]*Instituut voor Kern- en Stralingsfysica, KU Leuven, Celestijnenlaan 200D, B-3001 Leuven, Belgium*

[2]*Materials Department, University of California, Santa Barbara, California 93106-5050, USA*

[3]*Departement Fysica, Universiteit Antwerpen, Groenenborgerlaan 171, B-2020 Antwerpen, Belgium*

[4]*Laboratorium voor Vaste-Stoffysica en Magnetisme, KU Leuven, Celestijnenlaan 200D, B-3001 Leuven, Belgium*

[5]*Advanced Photon Source, Argonne National Laboratory, Argonne, Illinois 60439, USA*

[6]*Department of Geology, University of Illinois at Urbana-Champaign, Urbana, Illinois 61801, USA*

(Received 6 May 2013; revised manuscript received 26 June 2013; published 26 July 2013; corrected 4 October 2013)

We investigate the link between superconductivity and atomic vibrations in Nb_3Sn films with a thickness ranging from 10 to 50 nm. The challenge of measuring the phonon density of states (PDOS) of these films has been tackled by employing the technique of nuclear inelastic scattering by ^{119}Sn isotopes to reveal the Sn-partial phonon density of states. With the support of *ab initio* calculations, we evaluate the effect of reduced film thickness on the PDOS. This approach allows us to estimate the changes in superconducting critical temperature T_c induced by phonon confinement, which turned out to be limited to a few tenths of K. The presented method is successful for the Nb_3Sn system and paves the way for more systematic studies of the role of phonon confinement in Sn-containing superconductors.

DOI: 10.1103/PhysRevB.88.045437 PACS number(s): 74.25.Kc, 74.78.Na, 63.22.Np, 63.20.dk

I. INTRODUCTION

Conventional superconductivity is one of the most prominent examples of electron-phonon coupling in solids. In the framework of the BCS theory, the critical temperature T_c is intimately related to the phonon spectrum of the superconducting material[1] through the electron-phonon coupling constant λ. In turn, λ depends on the Eliashberg function $\alpha^2F(E)$, where $\alpha^2(E)$ is the electron-phonon coupling characteristic and $F(E)$ is the phonon density of states (PDOS). Since T_c is directly linked to λ, the precise shape of the PDOS determines the T_c of the superconductor. In the 1970s and 1980s, considerable efforts have been made to determine the shape of the Eliashberg function of different materials.[2,3] The electron-phonon coupling has specifically been studied in Nb_3Sn bulk crystal, Nb_3Sn being one of the conventional superconductors with the highest T_c (18 K). Phonon softening was observed at low temperature and has been widely studied in connection with superconductivity.[4–6] In particular, it has been shown that the superconducting gap could have an influence on the phonon linewidth. It was observed that the linewidth of acoustic phonons with an energy smaller than the superconducting gap decreases below T_c.[4] This effect could be used to estimate the strength of the electron-phonon coupling in Nb_3Sn and its influence on the phonon linewidth. Even though these studies were carried out on bulk materials, it always remained difficult to obtain α^2 and F separately.

During the last two decades, the investigation of superconductivity has moved towards nanoscaled and confined systems. In particular, electron confinement and electronic level quantization have attracted a lot of interest.[7–9] When the confinement is strong, i.e., for critical sizes smaller than the coherence length or the London penetration depth, the T_c and the critical field H_c can be significantly modified. However, both the electron density of states at the Fermi level *and* the phonon density of states play an important role in conventional superconductors. The influence of phonon confinement on superconductivity has been nicely illustrated by the work of Strongin *et al.*, who proposed to engineer the PDOS to manipulate T_c.[10] They postulated that proper "phonon engineering" would allow one to increase the T_c of superconductors such as Nb, Pb, and Nb_3Sn by more than 50%. This was supposed to be achieved by nanostructuring the superconductors, for example by forming ultrathin (a few nm) sheets of material. In general, phonon softening effects are expected to increase T_c in thin films or nanoparticles. However, in most cases, it turns out to be difficult to quantify this effect due to the lack of knowledge on the PDOS of these nanoscale objects.

There are in fact a few good reasons for the lack of understanding of the interplay between electron and phonon confinement. First, one needs to disentangle electron *and* phonon effects. This is partly due to the fact that electron tunneling experiments, which have been used to measure α^2F, are intrinsically influenced by electronic effects and do not allow an independent measure of F.[11] Another issue is that it is experimentally challenging to measure the PDOS of ultrathin films or nanostructures. Inelastic neutron scattering, which has traditionally been used to obtain the dispersion relations of bulk superconductors, cannot be applied due to the lack of scattering volume. Infrared or Raman scattering cannot cover the full energy spectrum of the PDOS and electron probes are, as mentioned, too sensitive to electronic effects or/and suffer from a limited probing depth.

The technique of nuclear resonant inelastic x-ray scattering (NRIXS), which is based on a phonon-assisted resonant excitation of a nuclear level in Mössbauer isotopes such as ^{57}Fe and ^{119}Sn,[12] has evolved in the last decade up to the point that experiments on a single atomic layer of material (at the ^{57}Fe resonance) can be carried out.[13] Achieving similar sensitivity at the ^{119}Sn resonance remains challenging, but it nevertheless opened up the possibility to measure the phonon density of states of Sn-containing *nanoscale* superconductors.

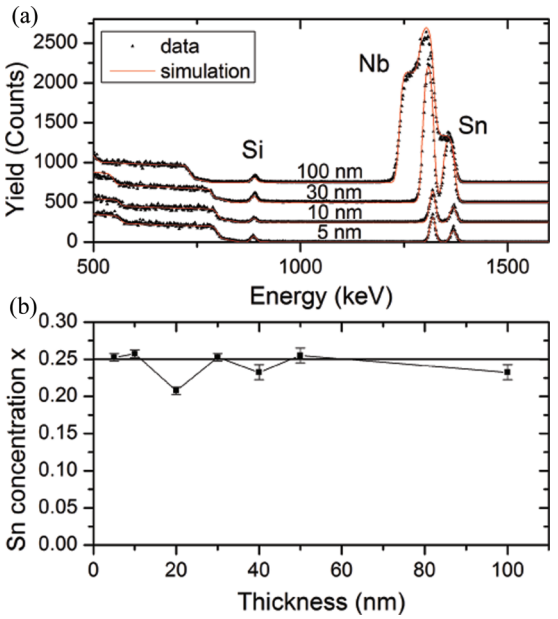

FIG. 1. (Color online) (a) RBS spectra recorded on Nb_3Sn films of different thicknesses. (b) Sn concentration in the $Nb_{1-x}Sn_x$ films.

In this article, we present a study of the lattice dynamics and superconducting properties of Nb_3Sn films as a function of the film thickness. The Sn-partial PDOS is measured at room temperature and at low temperatures (15 K, 25 K) by nuclear inelastic scattering. The experimental results are supported by *ab initio* calculations to obtain the full PDOS. We estimate the change in T_c which results from the phonon confinement using the McMillan expression. This approach allows us to clearly quantify the phonon contribution to the change in T_c in the Nb_3Sn films and demonstrate the power of the approach to study phonon effects in nanoscale superconductors.

II. SAMPLE PREPARATION AND STRUCTURAL CHARACTERIZATION

The Nb_3Sn films have been grown by molecular beam epitaxy co-deposition at 750 °C on MgO(100) substrates. The high deposition temperature is necessary to induce good superconducting properties of the Nb_3Sn films.[14] Nb was evaporated from a calibrated and ion flux monitored electron beam source, whereas isotopically enriched ^{119}Sn was evaporated from a calibrated Knudsen cell. Samples with thicknesses ranging from 5 to 100 nm were grown. All samples have been covered with a 8 nm Si layer to prevent oxidation in air.

The stoichiometry of each sample was investigated by Rutherford backscattering spectrometry (RBS). Figure 1(a) shows selected RBS spectra for different layer thicknesses. The Sn concentration x in the $Nb_{1-x}Sn_x$ films, shown in Fig. 1(b), is close to the desired value of 0.25 for most of the samples. The effect of off-stoichiometry on the lattice dynamics and superconductivity will be discussed below.

We used grazing incidence x-ray diffraction (XRD) measurements to investigate the crystalline quality of the samples. The incidence angle was set to 3°. Rietveld refinements[15] of the XRD patterns using the MAUD software[16] allowed us to

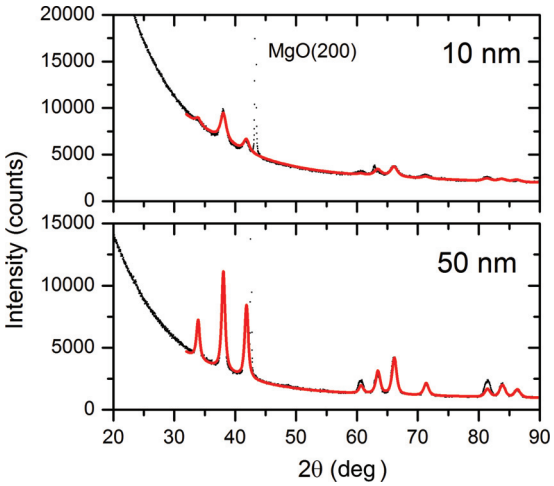

FIG. 2. (Color online) Grazing incidence x-ray diffraction patterns recorded on the 10 nm and 50 nm Nb_3Sn films. The solid red lines are fits resulting from the Rietveld refinement.

extract information about the crystallite size, i.e., the average coherently diffracting domain size, and texture of the samples. The patterns of the 10 nm and 50 nm samples, together with their fits, are shown in Fig. 2. The most obvious feature is the broadening of the XRD peaks for the 10 nm sample. The refinement procedure shows that the average crystal size is about 10 and 19 nm for the 10 and 50 nm thick layer, respectively. Since grazing incidence XRD has been used, the obtained crystallite sizes account for the average sizes along directions perpendicular to atomic planes which are not parallel to the sample surface. Therefore, this partially provides in-/out-of-plane structural characteristics. This means that the samples have small crystallites of maximum 20 nm size. The lattice parameters are found to be 0.5296 nm and 0.5285 nm for the 10 nm and 50 nm samples, very close to the bulk value of 0.5290 nm. The samples do not display strong texture, indicating that the grains are rather isotropically oriented. The nonappearance, in both samples, of the (110) superlattice peak at $2\theta = 24°$ shows that the alloy does not display long-range chemical ordering.

III. SUPERCONDUCTING PROPERTIES

The superconducting phase boundary of the samples was measured by SQUID magnetometry. The magnetic field was applied perpendicular to the sample surface. A typical phase boundary (for the 50 nm sample) is shown in Fig. 3(a). Figure 3(b) shows the T_c for the different samples. The Sn stoichiometry obtained from the RBS data is also plotted. For the two samples with the most deviating stoichiometry, i.e., the 20 and the 40 nm samples, a large drop in T_c is observed. This clearly illustrates the correlation between T_c and stoichiometry, which is well known for Nb_3Sn.[17] Indeed, Sn deficiency leads to a large drop of T_c as soon as the Sn concentration is below 0.23. A guide to the eye of the trend in T_c, ignoring the off-stoichiometric samples, is shown as a dashed line. According to this trend, T_c starts to drop significantly for thicknesses below 20 nm. Since we know from XRD that the crystallite size decreases drastically for layers thinner than 20

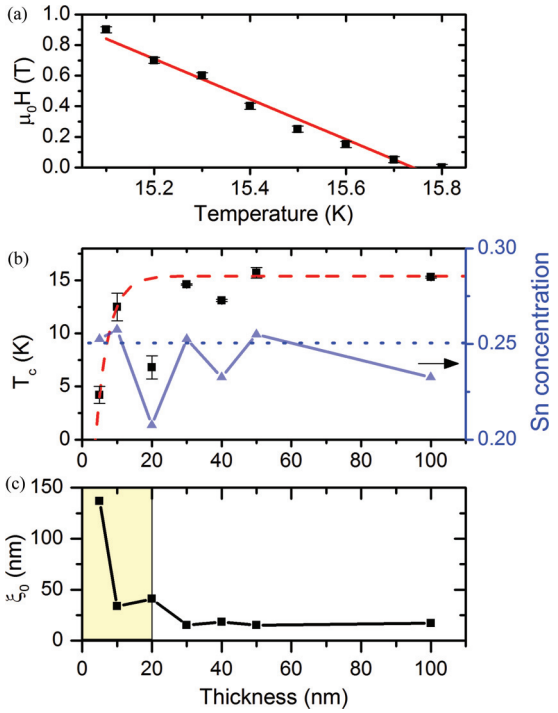

FIG. 3. (Color online) (a) Superconducting phase boundary for the 50 nm sample measured with SQUID magnetometry in a perpendicular field. (b) Evolution of T_c with thickness. The sudden drop in T_c corresponds to the samples with off-stoichiometric Sn concentration. The dashed red line is a guide to the eye. (c) Perpendicular superconducting coherence length $\xi(0)$. Thin-film effects start to appear below 20 nm.

nm, this behavior underscores the link between the crystallite size and T_c. From the slope of the phase boundary, we estimate the 0 K in-plane superconducting coherence length $\xi(0)$ using the following equation:

$$\xi(0) = \sqrt{\frac{\phi_0}{2\pi T_c d H_c/dT}}.$$

The result is shown in Fig. 3(c). $\xi(0)$ starts to increase significantly for layers thinner than or equal to 20 nm. It should be noted that although T_c for the 20 nm sample is smaller because of the off-stoichiometry, the coherence length does not change significantly yet. The departure from the bulk value for $\xi(0)$ appears once the sample thickness becomes equal to or smaller than $\xi(0)$ itself. This indicates a strong effect of the crystallite size on electron confinement.

IV. PHONON DENSITY OF STATES

The goal of the PDOS measurements is to relate the observed phonon confinement to the change in T_c. With this information, it will become possible to quantify the role of electrons and phonons on the evolution of T_c. Since the nuclear inelastic scattering technique is only sensitive to the Sn partial PDOS, *ab initio* calculations have been used to obtain the full PDOS as well as the Sn-partial PDOS.

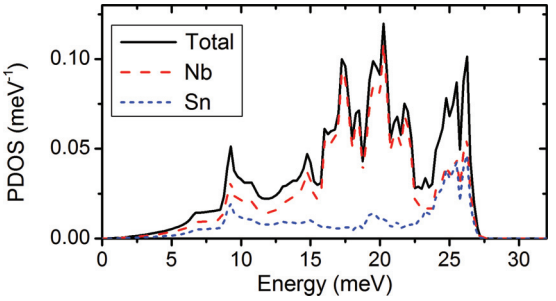

FIG. 4. (Color online) Partial and total phonon density of states obtained from the *ab initio* calculations.

A. *Ab initio* calculations

We performed *ab initio* calculations using the ABINIT[18] package. A plane-wave basis has been used with Troullier-Martins pseudopotentials[21] and the local-density approximation (LDA) as the exchange-correlation potential. A 4×4×4 Monkhorst-Pack[19] grid was used to sample the Brillouin zone. Phonons were calculated within density-functional perturbation theory.[20] The PDOS was obtained on a Fourier interpolated $40\times40\times40k$-point grid. The PDOS was separated in a Nb and Sn contribution as shown in Fig. 4. This will be used to compare with the NRIXS data which provide only the Sn-partial PDOS. After comparison with the experiment, these calculated PDOS will be used to estimate the T_c.

B. Nuclear inelastic scattering

The Sn partial PDOS have been measured by NRIXS. The preliminary feasibility experiments were carried out at the ID22N nuclear resonance outstation of the European Synchrotron Radiation Facility.[22] However, the measurements which are presented here have been done at sector 3-ID of the Advanced Photon Source.[12] The high-resolution monochromator had a resolution of 1 meV.[23] We used a grazing incidence scattering geometry with an incident angle set below 1° to maximize the signal in the inelastic detector. To match the sample footprint in grazing incidence, the beam was focused down to 10 μm using Kirkpatrick-Baez mirrors. Measurements have been carried out at room temperature for the full series of samples and at 15 and 25 K for the 10 nm and 50 nm samples. The low temperature experiments have been carried out in a He-flow cryostat.

The PDOS measured at room temperature are shown in Fig. 5. The overall shape of the PDOS remains similar for all thicknesses. The main systematic change is a gradual decrease of the intensity of the optical phonon mode at 25 meV. Such a decrease of the high energy phonon modes is often observed in metallic nanostructures or surfaces.[13,24,25] To quantify this effect in detail, we will use the input of the theoretical calculations presented in the previous subsection.

In the following, we consider the 50 nm sample as a "bulk" reference, since it is reasonably thick and has better stoichiometry than the 100 nm sample. If we overlay the measured PDOS for the 50 nm sample with the theoretical curve, we see that the experimental spectra show much broader features, as shown in Fig. 6. In the NRIXS experiment, the experimental resolution function is given by the energy spectrum

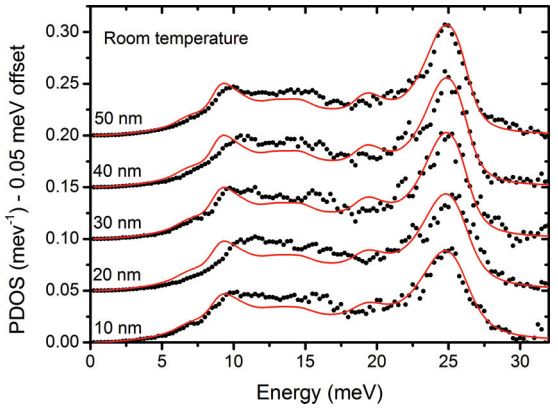

FIG. 5. (Color online) Phonon densities of states recorded at room temperature for Nb_3Sn films of different thicknesses. The red solid lines are the theoretical result after application of the damped harmonic oscillator model as explained in the text.

of the photons after the high-resolution monochromator. In our experiment, the resolution was close to 1 meV full width at half maximum. The convolution of the theoretical curve with the resolution function should in principle reproduce the measured spectra. However, at the peak around 25 meV the correspondence between calculations and experiment is not very good, as shown in Fig. 6. The peak in the theoretical curve is shifted slightly to higher energy and still narrower than the experimental data. Here, we hit one of the limitations of *ab initio* calculations, which use the harmonic approximation to calculate the phonon spectrum. This implies an infinite phonon lifetime. In a real system, this lifetime will be reduced due to various factors such as the anharmonicity of the atomic potential, the presence of defects, boundaries, and electron-phonon coupling. Thus, a more appropriate way to compare theory with experiment is to introduce a finite phonon lifetime. This point will be discussed in more detail for a

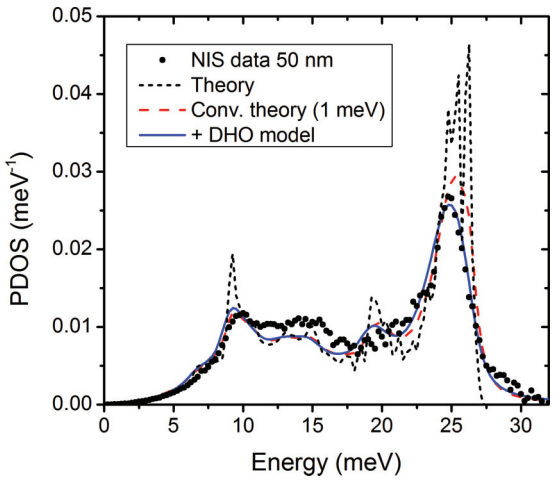

FIG. 6. (Color online) Comparison of the experimentally measured PDOS at 300 K with the raw theoretical calculation and the result of convolution with a 1 meV resolution function. The result of the application of the damped harmonic oscillator (DHO) model is also shown.

variety of systems.[26] The effect of finite phonon lifetime can be approximated by applying a damped harmonic oscillator (DHO) model to the *ab initio* calculated phonon spectrum.[27] This phenomenological model describes the "damping" of the phonons; i.e., it provides a finite phonon lifetime, which leads to a broadening of the phonon lines. Mathematically, this process is described as a convolution of the original PDOS with an appropriate broadening function $D(E,E^*)$:

$$F_{\mathrm{DHO}}(E^*) = \int D(E,E^*)F(E)dE. \tag{1}$$

In the case of a phonon lifetime decrease, it has been shown that the damped harmonic oscillator function is a good choice for $D(E,E^*)$:[27,29]

$$D(E,E^*) = \frac{1}{\pi Q E^*}\frac{1}{\left(\frac{E^*}{E}-\frac{E}{E^*}\right)^2+\frac{1}{Q^2}}, \tag{2}$$

where Q is the quality factor, which describes the number of periods a phonon will remain in a given state. Hence, the lower the value of Q, the shorter the lifetime and the larger the broadening. This function is essentially a Lorentzian with a width that increases with E^*, meaning that the PDOS features become broader at higher energy. The final PDOS to be compared to our experimental data is thus constructed by convolution of the theoretical PDOS with the DHO function in Eq. (2). The experimental resolution function is then convoluted with the resulting spectrum to reproduce the actual measurement conditions. In this model, only the Q factor is adjusted to provide the best match between the theoretical and experimental PDOS. The result for the 50 nm film is shown in Fig. 6. A very good match between theory and experiment is found for $Q = 23$.

We have applied the DHO model to fit all the recorded PDOS. The result is shown as the solid red lines in Fig. 5. The extracted Q factors (Fig. 8) give a measure of the evolution of the phonon lifetime as a function of film thickness. One can notice that the PDOS and the obtained Q do not strongly depend on the film stoichiometry. This means that the change in T_c observed for off-stoichiometric films does not correlate with a change of the phonon spectrum. Hence, the off-stoichiometry seems to affect mainly the electron density of states rather than the PDOS.

There are a number of factors that can affect the phonon lifetime in solids. Anharmonicity in the atomic potential is

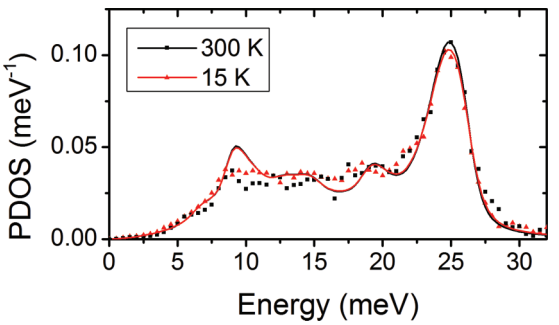

FIG. 7. (Color online) PDOS of the 50 nm sample recorded at 15 K and 300 K. The lines are theoretical calculations convoluted using the DHO model.

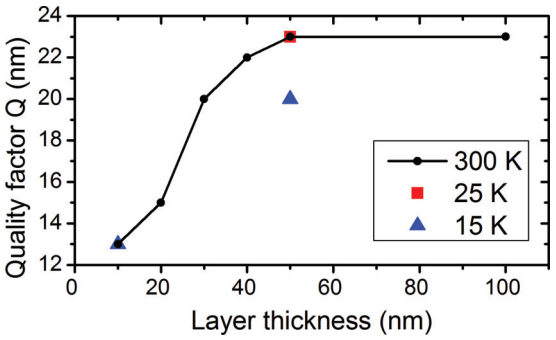

FIG. 8. (Color online) Quality factor Q obtained by fitting the experimental Sn partial PDOS with the theoretical curves.

typically expected to decrease the lifetime. However, this process is temperature dependent and a stronger damping should occur as the temperature is increased.[28] We have measured the PDOS at 15 K and 25 K for the 50 nm and 10 nm samples. The typical differences between 25 K and 15 K is shown for the 50 nm film in Fig. 7. The corresponding Q values are shown in Fig. 8. These Q values are equal to or even smaller than those obtained at room temperature. This clearly speaks against anharmonic effects to be responsible for the observed broadening. Another source of reduction in the phonon lifetime originates from a smaller grain size. The DHO model has been used to describe size effects in metal nanostructures.[29,30] Indeed, the lifetime in nanostructures is expected to decrease due to the smaller mean-free path induced by the smaller crystallite size. In Fig. 8, we observe that Q starts to decrease already for thicknesses below 50 nm. Since the crystallite size ($\sim$20 nm) is much smaller than this film thickness, we expect that the decrease of Q (which occurs without a significant decrease of the crystallites size) is indicative of the presence of more defects in the film as the thickness decreases. Finally, electron-phonon coupling effects, which are known to have a strong influence on the phonon linewidth in Nb_3Sn,[4,5] could not be quantified in this study. It is presently not possible to achieve a low enough temperature without compromising the measurement scheme for NRIXS. However, at this stage we believe that the increased damping observed for thinner films is most likely not related to a change in the electron-phonon coupling properties of the film but rather due to the decreasing grain size or the increase of defects within the film. Even though the grain size is already as small as 10 nm (for the 10 nm sample), we see only a limited change in the phonon spectrum. We can thus expect that phonon effects are not likely to have a large influence on T_c.

As shown in Fig. 7 for the 50 nm sample, there is a slight decrease of the intensity of the optical phonon peak at 15 K compared to the 25 K measurement, which leads to a decrease of the quality factor used in the DHO model, as shown in Fig. 8. The low-energy part of the spectrum also becomes softer and matches better the theoretical prediction. It is rather surprising that this softening and decrease of Q appears only at 15 K while the 25 K PDOS is closer to the room temperature one. It should be noted that 15 K is just below the measured T_c of the 50 nm sample. However, it was not possible to check *in situ* whether the sample was effectively in the superconducting state. We can thus not establish if the observed change in PDOS is connected to superconductivity and to the modification of the phonon linewidth reported by Axe and Shirane.[4] The PDOS of the 10 nm sample at 15 and 25 K does not display any change compared to the room temperature curve, the reason why they all have the same Q in Fig. 8.

V. DISCUSSION

With the obtained PDOS, we can calculate how the decreased phonon lifetime affects T_c. For that purpose, we use the formalism outlined by Markiewicz,[31] which is based on the McMillan expression for λ:

$$\lambda = 2\int \frac{\alpha^2(E)F(E)}{E}dE. \tag{3}$$

T_c is then defined as

$$T_c = \frac{0.25\langle\Omega^2\rangle^{1/2}}{(e^{2/\lambda_{\text{eff}}}-1)^{1/2}}, \tag{4}$$

where λ_{eff} depends on λ, which is calculated from Eq. (3). $\langle\Omega^2\rangle$ is the characteristic phonon frequency defined by

$$\langle\Omega^2\rangle = \frac{2}{\lambda}\int \alpha^2(E)F(E)EdE. \tag{5}$$

In order to calculate T_c using the theoretical PDOS for $F(E)$, we thus only need to fix the shape of $\alpha^2(E)$, which is approximated in Nb_3Sn by an exponential decay of the form[31]

$$\alpha^2(E) = \alpha_0^2 e^{-E/E_0}. \tag{6}$$

Regardless of the exact value of α_0^2 and E_0, this equation essentially tells us that the soft modes will have a larger weight than the high-energy modes. It should be noted that $\alpha^2(E)$ is not determined in a direct way but rather obtained by calculating the ratio between a PDOS measured by neutron scattering and an Eliashberg function α^2F measured by electron tunneling on different samples.[32,33] There is in general still uncertainty on the precise shape of $\alpha^2(E)$.

As input for Eqs. (3) and (6), we use the calculated PDOS for Nb_3Sn (not the partial PDOS), onto which the DHO model with the appropriate Q determined from fitting the partial PDOS is applied. The other parameters are fixed to the values used by Markiewicz and represent bulk properties; i.e., $\alpha_0^2 =$ 35 meV, $E_0 = 13$ meV, and $\mu^* = 0.157$. The result shown in Fig. 9 indicates that the phonon damping effects contribute to a decrease of T_c of as much as 0.35 K for the 10 nm sample, compared to the thick film. This phonon-induced decrease of T_c (calculated T_c) is compared with the T_c measured by SQUID in Fig. 9. We also show the experimental T_c from which phonon effects are subtracted, which clearly present the relatively low impact of the phonons on the measured T_c.

With the latter development, we have isolated the contribution of phonons to the change in T_c in the Nb_3Sn films. This contribution is relatively small in the studied thickness range, which indicates that electronic confinement is predominant. However, the presented result allows us to observe in a direct and clear way the contribution of the phonons on T_c. The results also show that the effect of reduced dimensions on the phonon spectrum does not necessarily lead to an increase of T_c. Whether T_c will increase or not will depend on how the phonon spectrum is modified but also on which part of the spectrum

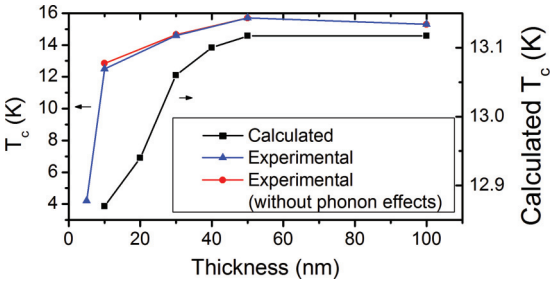

FIG. 9. (Color online) T_c calculated using the McMillan formula using the theoretical calculations convoluted with the appropriate DHO function. Phonon damping results in a decrease in T_c of as much as 0.35 K for the 10 nm sample. The SQUID recorded T_c is shown together with an hypothetical correction induced by the phonons. This clearly shows that phonon damping effects play only a minor role in the observed decrease of T_c.

contributes more effectively to the electron-phonon coupling, i.e., what is the shape of α^2. As such, this work also highlights the importance of an accurate determination of α^2, in addition to accurate PDOS measurements. Only by decoupling these terms in the Eliashberg function $\alpha^2 F$, one can assess whether α^2 is modified in nanostructured superconductors.

VI. CONCLUSIONS

We have investigated the relationship between film thickness, superconductivity, and phonon density of states in Nb_3Sn films. The PDOS measurements show a damping of the high-energy phonon modes in the thinner films. This effect can be reproduced by applying a damped harmonic oscillator model to the theoretical PDOS obtained by *ab initio* calculations. This broadening is expected to be due to the decreasing grain size and/or increasing number of defects in the thinner films. Thanks to the good match of theory and experiment for the Sn partial PDOS, we can use the calculated full PDOS to estimate the change in T_c solely due to the phonon effects in the thin film. We observed that these changes induce a decrease of the T_c with decreasing film thickness which is moderate compared to the observed change in T_c. Our findings allow us to separate and quantify the role of both phonon and electron confinement effects, the latter of which are in this case more prominent. The method for obtaining the PDOS and comparing with theory proves efficient to evaluate the role of phonons in nanoscale superconductivity. As such, new experiments can be envisioned, based on the ^{119}Sn resonance, to study phonon effects in Sn-containing superconductors.

ACKNOWLEDGMENTS

The authors would like to cordially thank Dr. Rudolf Rüffer from the nuclear resonant scattering group of the ESRF for the support and gratefully acknowledge the ESRF for providing beamtime for the preliminary phonon study. S.C., K.H., and E.M. thank the Flemish Science Foundation (FWO-Vl) for their personal fellowship. This work was supported by FWO-Vl, the Methusalem program of the Flemish government, and the Concerted Research Action program (GOA/09/006) and (GOA/14/007). Use of the Advanced Photon Source, an Office of Science User Facility operated for the U.S. Department of Energy (DOE) Office of Science by Argonne National Laboratory, was supported by the U.S. DOE under Contract No. DE-AC02-06CH11357.

*sebastien.couet@fys.kuleuven.be

[1]W. L. McMillan, Phys. Rev. **167**, 331 (1968).
[2]J. P. Carbotte, Rev. Mod. Phys. **62**, 1027 (1990).
[3]J. M. Rowell, W. L. McMillan, and W. L. Feldmann, Phys. Rev. B **3**, 4065 (1971).
[4]J. D. Axe and G. Shirane, Phys. Rev. Lett. **30**, 214 (1973).
[5]J. D. Axe and G. Shirane, Phys. Rev. B **28**, 4829 (1983).
[6]L. Pintschovius, H. Takei, and N. Toyota, Phys. Rev. Lett. **54**, 1260 (1985).
[7]J. von Delft, Ann. Phys. **10**, 1 (2001).
[8]A. A. Shanenko, M. D. Croitoru, and F. M. Peeters, Phys. Rev. B **75**, 014519 (2007).
[9]S. Bose, A. M. Garcia-Garcia, M. M. Ugeda, J. D. Urbina, C. H. Michaelis, I. Brihuega, and K. Kern, Nat. Mater. **9**, 550 (2010).
[10]M. Strongin, O. F. Kammerer, J. E. Crow, R. D. Parks, D. H. Douglass, and M. A. Jensen, Phys. Rev. Lett. **21**, 1320 (1968).
[11]I. Giaever, Rev. Mod. Phys. **46**, 245 (1974).
[12]E. E. Alp, W. Sturhahn, T. S. Toellner, J. Zhao, M. Hu, and D. E. Brown, Hyperfine Interact. **144-145**, 3 (2002).
[13]T. Slezak, J. Lazewski, S. Stankov, K. Parlinski, R. Reitinger, M. Rennhofer, R. Rüffer, B. Sepiol, M. Slezak, N. Spiridis, M. Zajac, A. I. Chumakov, and J. Korecki, Phys. Rev. Lett. **99**, 066103 (2007).
[14]T. P. Orlando, E. J. McNiff, S. Foner, and M. R. Beasley, Phys. Rev. B **19**, 4545 (1979).
[15]R. A. Young, *The Rietveld Method*, International Union of Crystallography (Oxford University Press, Oxford, 1995).
[16]L. Lutteroni and P. Scardi, J. Appl. Crystallogr. **23**, 246 (1990).
[17]A. Godeke, Supercond. Sci. Technol. **19**, R68 (2006).
[18]X. Gonze, B. Amadon, P. M. Anglade, J.-M. Beuken, F. Bottin, P. Boulanger, F. Bruneval, D. Caliste, R. Caracas, M. Cote, T. Deutsch, L. Genovese, Ph. Ghosez, M. Giantomassi, S. Goedecker, D. Hamann, P. Hermet, F. Jollet, G. Jomard, S. Leroux, M. Mancini, S. Mazevet, M. J. T. Oliveira, G. Onida, Y. Pouillon, T. Rangel, G.-M. Rignanese, D. Sangalli, R. Shaltaf, M. Torrent, M. J. Verstraete, G. Zérah, and J. W. Zwanziger, Comput. Phys. Commun. **180**, 2582 (2009).
[19]H. J. Monkhorst and J. D. Pack, Phys. Rev. B **13**, 5188 (1976).
[20]S. Baroni, S. de Gironcoli, A. Dal Corso, and P. Giannozzi, Rev. Mod. Phys. **73**, 515 (2001).
[21]N. Troullier and José Luriaas Martins, Phys. Rev. B **43**, 1993 (1991).
[22]R. Rüffer and A. I. Chumakov, Hyperfine Interact. **97-98**, 589 (1996).
[23]T. S. Toellner, M. Y. Hu, G. Bortel, W. Sturhahn, and D. Shu, Nucl. Instrum. Methods Phys. Res., Sect. A **557**, 670 (2006).
[24]S. Stankov, Y. Z. Yue, M. Miglierini, B. Sepiol, I. Sergueev, A. I. Chumakov, L. Hu, P. Svec, and R. Rüffer, Phys. Rev. Lett. **100**, 235503 (2008).

[25]B. Roldan Cuenya, W. Keune, R. Peters, E. Schuster, B. Sahoo, U. von Hörsten, W. Sturhahn, J. Zhao, T. S. Toellner, E. E. Alp, and S. D. Bader, Phys. Rev. B **77**, 165410 (2008).
[26]S. Couet *et al*. (unpublished).
[27]B. Fultz, Prog. Mater. Sci. **55**, 247 (2010).
[28]X. Tang, C. W. Li, and B. Fultz, Phys. Rev. B **82**, 184301 (2010).
[29]R. Röhlsberger, W. Sturhahn, T. S. Toellner, K. W. Quast, P. Hession, M. Hu, J. Sutter, and E. E. Alp, J. Appl. Phys. **86**, 584 (1999).
[30]S. Stankov, R. Röhlsberger, T. Slezak, M. Sladecek, B. Sepiol, G. Vogl, A. I. Chumakov, R. Rüffer, N. Spiridis, J. Lazewski, K. Parlinski, and J. Korecki, Phys. Rev. Lett. **99**, 185501 (2007).
[31]W. D. Markiewicz, Cryogenics **44**, 767 (2004).
[32]J. K. Freericks, A. Y. Lin, A. Quandt, and J. Geerk, Phys. Rev. B **65**, 224510 (2002).
[33]J. Geerk, U. Kaufmann, W. Bangert, and H. Rietschel, Phys. Rev. B **33**, 1621 (1986).